# Ab Initio and DFT Modeling of Stereoselective Deamination of Aziridines by Nitrosyl Chloride

**ANBARASAN KALAISELVAN,[1] PONNAMBALAM VENUVANALINGAM,[1] JORDI POATER,[2] MIQUEL SOLÀ[2]**

[1]*Department of Chemistry, Bharathidasan University, Tiruchirappalli-620 024, India*

[2]*Institut de Química Computacional and Departament de Química, Universitat de Girona, 17071 Girona, Catalonia, Spain*

*Received 11 June 2004; accepted 28 June 2004*
*Published online 17 November 2004 in Wiley InterScience (www.interscience.wiley.com).*
*DOI 10.1002/qua.20364*

**ABSTRACT:** The stereochemical course of the deamination of cis-2,3-dimethylaziridine by nitrosyl chloride was investigated at the QCISD/6-31G(d) level. Calculations reveal that the reaction takes place in two steps. In the first step, the reactants form a pre-reactive complex, followed by a spiro-type bicyclic transition state, which on dissociative cycloelimination gives the N-nitrosoaziridine intermediate. In the second step, this intermediate undergoes cycloreversion through a slightly asynchronous concerted transition state to form an alkene with the same stereochemistry, which is in total agreement with experiment. In the whole reaction, the denitrosation step is found to be rate-determining. For comparison, geometry optimizations and energies were also obtained at the B3LYP/6-31G(d) level. It was found that the B3LYP energy results differed significantly from the QCISD ones. To analyze the reason for this difference, B3LYP calculations were repeated by varying the

*Correspondence to:* P. Venuvanalingam; e-mail: venuvanalingam@yahoo.com

Contract grant sponsor: UGC, India.
Contract grant number: 12-30/2002 (SR-1) dt 21st May, 2002.
Contract grant sponsor: Spanish McyT.
Contract grant numbers: BQU2002-0412-C02-02, BQU2002-03334.
Contract grant sponsor: Departament d'Universitats, Recerca i Societat de la Informació of the Generalitat de Catalunya, Distinguished University Research Promotion 2001 (to M.S.).
This article contains supplementary material available via the Internet at http://www.interscience.wiley.com/jpages/0020-7608/suppmat.

contribution of exact exchange in the Becke functional. With respect to the QCISD results, it has been shown that the functional with 0% exact exchange yields the best activation barriers, whereas the functional with 30% exact exchange is the most suitable one to carry out the complexation and reaction energy calculations.  Int J Quantum Chem 102: 139–146, 2005

**Key words:** deamination; ring opening; aziridines; ab initio; DFT; PS-B3LYP calculations

## Introduction

Olefin inversion is one of the techniques normally employed to create double bonds with definite stereospecificity, and this can be done in several ways [1]. Olefin inversion through aziridine synthesis and subsequent deamination is one of them. The outstanding characteristic of aziridine is its high reactivity toward a wide variety of electrophilic and nucleophilic reagents; this tendency of aziridines is due to high ring strain [2]. Aziridine chemistry is mainly dominated by a ring opening reaction, and it has widespread applications in synthesizing biologically important active species including alkaloids, amino acids, and $\beta$-lactam antibiotics [3]. Aziridines can be deaminated by nitrosating it with nitrosyl chloride or nitromethane or 3-nitro-N-nitrosocarbazole and denitrosating it. In the reaction with NOCl the alkene produced is 99% cis deaminated [1, 4]. Clark and Helmkamp [4] studied the deamination of stereoisomers of 2,3-dimethylaziridines by NOCl and the products obtained were found to be completely stereospecific. They isolated an N-nitroso derivative as an intermediate.

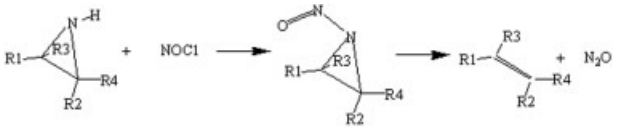


The mechanism of this reaction still remains unexplored and, therefore, here we have traced the reaction pathway of deamination of cis-2,3-dimethylaziridine and through that explain the stereospecificity of the reaction. We present a theoretical study of the mechanism of this reaction by using both Density Functional Theory (DFT) and configuration interaction (CI) levels of theory. We show that the B3LYP results differ significantly from those obtained at the QCISD level of theory, taken as reference for its higher accuracy. This is the reason why this study is complemented by a series of calculations to discuss the effect of varying the fraction of exact HF exchange ($a_0$) included in the hybrid B3LYP functional.

The B3LYP method uses three parameters, $a_o$, $a_x$, $a_c$, which were determined by Becke [5] by a linear least-squares fit to 56 experimental atomization energies, 42 ionization potentials, and 8 proton affinities. The values thus obtained were $a_o = 0.20$, $a_x = 0.72$, and $a_c = 0.81$. Looking for improved results, attempts were made to perform calculations by changing these values internally. Latajka et al. [6] were the first who changed the $a_o$ value from 0.2 to 0.35 in the B3P86 functional to better describe the structural properties of hydrogen-bonded complexes. Since then, a number of articles have addressed the effect of varying the $a_o$ parameter of the B3LYP functional on molecular structure [7–10], vibrational frequencies [9], first-order density [11, 12], thermochemistry and energy barriers [7, 13–16], ionization potentials [17], hydrogen bond infrared signature [18], and nuclear resonance shielding constants [19]. These authors have shown that a routine calculation with a B3LYP level that includes 20% exact exchange is not the most suitable in all cases, and sometimes better Becke-derived functionals with varying contributions of exact exchange may be tried. We attempted this for our reaction and compared it with our QCISD results [20].

## Computational Details

Geometry optimizations were carried out with the QCISD method [20] and the DFT methodology by means of the B3LYP hybrid functional – Becke's three-parameter [5] nonlocal exchange functional with the nonlocal correlation functional of Lee, Yang, and Parr [21], using the Gaussian 98 program [22]. The 6-31G(d) basis set was used throughout [23]. All stationary points found, except those obtained at the QCSID level, were characterized as

either minima or transition states (TSs) by computing the vibrational harmonic frequencies; TSs have a single imaginary frequency while minima have all real frequencies. All B3LYP/6-31G(d) TSs were further characterized by animating the imaginary frequency in MOLDEN [24] by intrinsic reaction coordinate (IRC) analysis. Bond orders reported here are Wiberg [25] bond indices calculated by the natural bond orbital (NBO) program [26]. From these bond orders, bond formation index $BF_i^{A_k}$ and bond cleavage index $BC_j^{A_k}$ for $A_k$ species (k = 1 to 6) are calculated as follows [27]:

$$BF_i^{A_k} \text{ or } BC_j^{A_k} = \frac{BO_{i\,or\,j}^{A_k} - BO_{i\,or\,j}^{R}}{BO_{i\,or\,j}^{P} - BO_{i\,or\,j}^{R}} \times 100 \qquad (1)$$

$BFC_{Ave}^{Ak}$is the average percentage of all bonds forming and cleaving indices for a given $A_k$ species in the reaction path, according to the following expression:

$$BFC_{Ave}^{A_k} = \frac{\sum_{i,j}(BF_i + BC_j)}{n}, \qquad (2)$$

where $n$ is the total number of bonds that undergo major changes during the reaction. The superscripts R and P in Eq (1) refer to reactants and products respectively.

In the Gaussian 98 [22] implementation, the expression of the B3LYP functional is [28]:

$$E_{XC} = E_X^{LSDA} + a_o(E_X^{exact} - E_X^{LSDA}) + a_x\Delta E_X^{B88} + E_C^{VWN} + a_c(\Delta E_C^{LYP} - E_C^{VWN}) \qquad (3)$$

with the $E_X^{\text{exact}}$, $E_X^{\text{LSDA}}$, $\Delta E_X^{\text{B88}}$, and $\Delta E_C^{\text{LYP}}$ terms being the HF exchange energy based on Kohn-Sham orbitals, the uniform electron gas exchange-correlation energy, Becke's 1988 gradient correction for exchange [29], and Lee-Yang-Parr's gradient correction to correlation [21], respectively. To obtain a deeper insight into the reason behind the B3LYP failure in describing this reaction, we carried out the same above calculations but varied monotonically the proportion of exact exchange introduced. We made use of the Gaussian 98 [22] program feature that allows one to vary the B3LYP standard Becke's parameter set (PS) through internal options [7, 12]. We changed the $a_o$ parameter by 0.100 increments in the interval $0.100 \leq a_o \leq 0.900$, with fixed $a_x = 1 - a_o$ and $a_c = a_x$. The $a_x = 1 - a_o$ relationship has been used in some hybrid functionals, such as the B1 method [30], which in addition takes $a_c = 1$ and $a_o = 0.16$ or 0.28 depending on the choice of the nonlocal exchange correction. We also found in previous works that the $a_x = 1 - a_o$ and $a_c = a_x$ relationships between the B3LYP parameters are, on average, the optimal ones to minimize the difference between the actual B3LYP density and the QCISD one in a series of small molecules [12], and for this reason the $a_x = 1 - a_o$ and $a_c = a_x$ relationships will be maintained throughout this work. However, neither the choice employed here nor other possible alternative relations among the three parameters should be considered universal. These PS-B3LYP calculations are further compared with HF and QCISD ab initio calculations for all species with the same 6-31G(d) basis set.

## Results and Discussion

Nitrosyl chloride reacts with cis-2,3-dimethylaziridines to form cis-2-butenes with 100% stereospecificity through the formation of N-nitrosoaziridine as an intermediate. Reaction steps are depicted in Figure 1, the energy profile is presented in Figure 2, and optimized structures are shown in Figure 3. According to frontier orbital energy (FOE) values, the initial interaction between the cis-2,3-dimethylaziridine and NOCl is mainly controlled by the HOMO of aziridine (A1) and the LUMO of NOCl interaction (the LUMO(NOCl)-HOMO(Azir) and the LUMO(Azir)-HOMO(NOCl) energy gaps are 11.0 and 18.0 eV at the QCISD/6-31G(d) level of theory, and 2.2 and 10.7 eV with the B3LYP/6-31G(d) method). NOCl adds on to aziridine concertedly across the N–H bond of aziridine (A1) to form TS1 (A3) via a pre-reactive complex (A2). The complex (A2) has a stabilization energy of 5.35 kcal · $mol^{-1}$. TS1 eliminates one molecule of HCl to form N-nitrosoaziridine (A4). The formation of N-nitrosoaziridine and HCl has been confirmed experimentally [4]. The HCl formed has been reported to form aziridine hydrochloride, and N-nitrosoaziridine has been isolated as a yellow oil at low temperature and has been found to be stable at low temperatures.

The N-nitroso intermediate (A4) undergoes cycloreversion concertedly through a transition state TS2 (A5) to form the final alkene (A6) by eliminating one molecule of $N_2O$. Deamination of aziridine using NOCl is therefore found to take place in two steps: first, the formation of the N-nitrosoaziridine intermediate (A4); and second, decomposition of

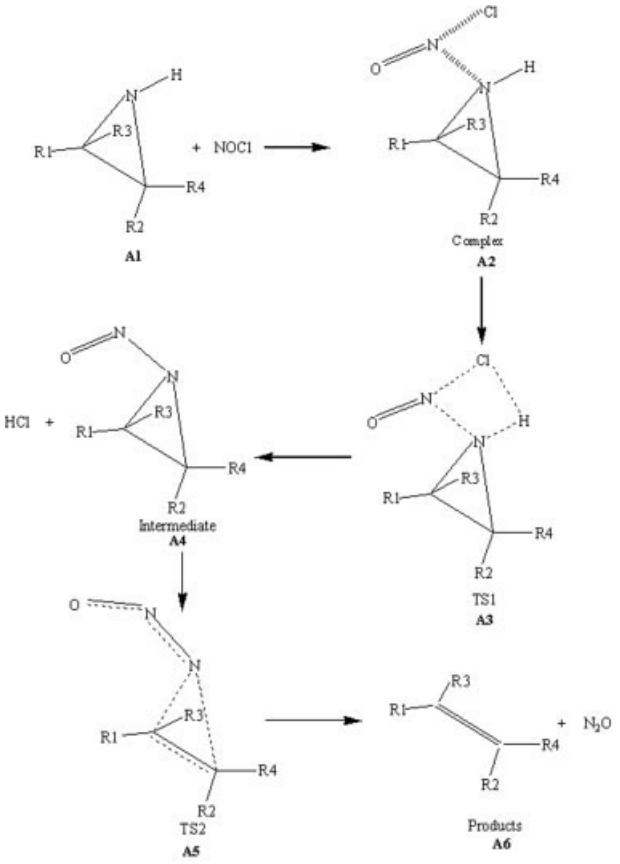


**FIGURE 1.** Scheme for the deamination of cis-2,3-dimethylaziridine with NOCl.

the N-nitroso intermediate (A4) into the final product alkene (A6). The energy profile presented in Figure 2 shows that the second step is rate-determining, the activation energy for this step being 31.09 kcal · $mol^{-1}$ and 48.81 kcal · $mol^{-1}$ at the QCISD and B3LYP levels, respectively.

### Geometry of the Transition States and Intermediates

In close encounter reactants form a pre-reactive complex (A2) and in that N–Cl bond weakens and a weak N–N bond is formed. This is further strengthened in TS1 (A3). Additionally, in TS1 the N–H bond in aziridine weakens and the H–Cl bond develops. In the N-nitrosoaziridine intermediate (A4) the N–N bond is completely formed and HCl separates. In TS2 (A5) both C–N bonds of nitrosoaziridine cleave somewhat asynchronously and the N–N bond develops into an N–N double bond. The slight asynchronous nature of the C–N bonds cleavage in TS2 is due to spatial disposition of the N–O bond towards one C–N bond of aziridine. An interesting observation in the geometry of the reaction path scan is that TS1 has a distorted spiro structure (in A3 the dihedral angles ∠N14N3C2C1 and ∠H16N3C2C1 are –108.7° and 107.3°, respectively) and that TS2 shows concerted elimination of $N_2O$, as suggested from experiments.

### Bond Order Analysis

Computed bond indices $BF_i$ or $BC_j$ listed in Table I show that the pre-reactive complex formed (A2) is very weak and bond indices are very low, the N–N bond is formed only around 1%, and the N–Cl bond in NOCl is 6% cleaved. In the TS1 (A3), the N–N and H–Cl bonds are formed to 17–30%, while N–Cl bond cleaves to 93%. In N-nitrosoaziridine (A4) the N–N single bond is fully formed, but the percentage of bond formed is indicated as 41%, as it is expressed relative to the N=N bond formed in the final product. In the intermediate (A4), N–H in aziridine and N–Cl in NOCl cleave totally and the N–O bond of NOCl cleaves partially (38%). In TS2 (A5), at the QCISD level, the alkene bond is formed up to 98% and the cleavage of the C–N bond takes place almost synchronously. In contrast, B3LYP calculations indicate that the alkene bond is formed only to 28% and the asynchronicity in the C–N bond cleavage is very high—one bond cleaving up to 65% and another by 31%, i.e.,

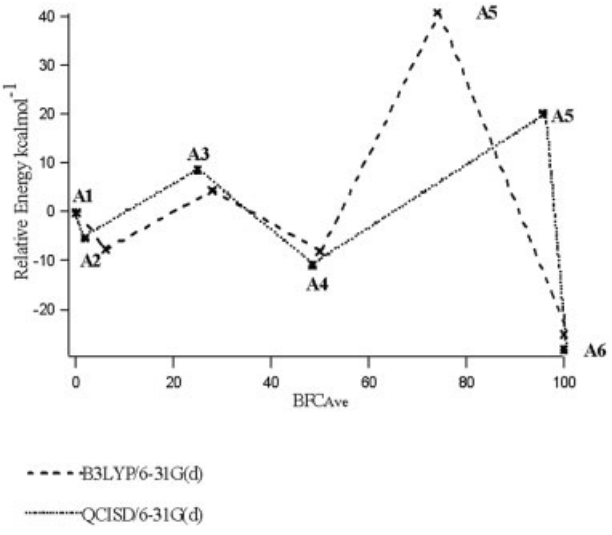


**FIGURE 2.** Energy profile for the deamination of cis-2,3-dimethylaziridines with NOCl.

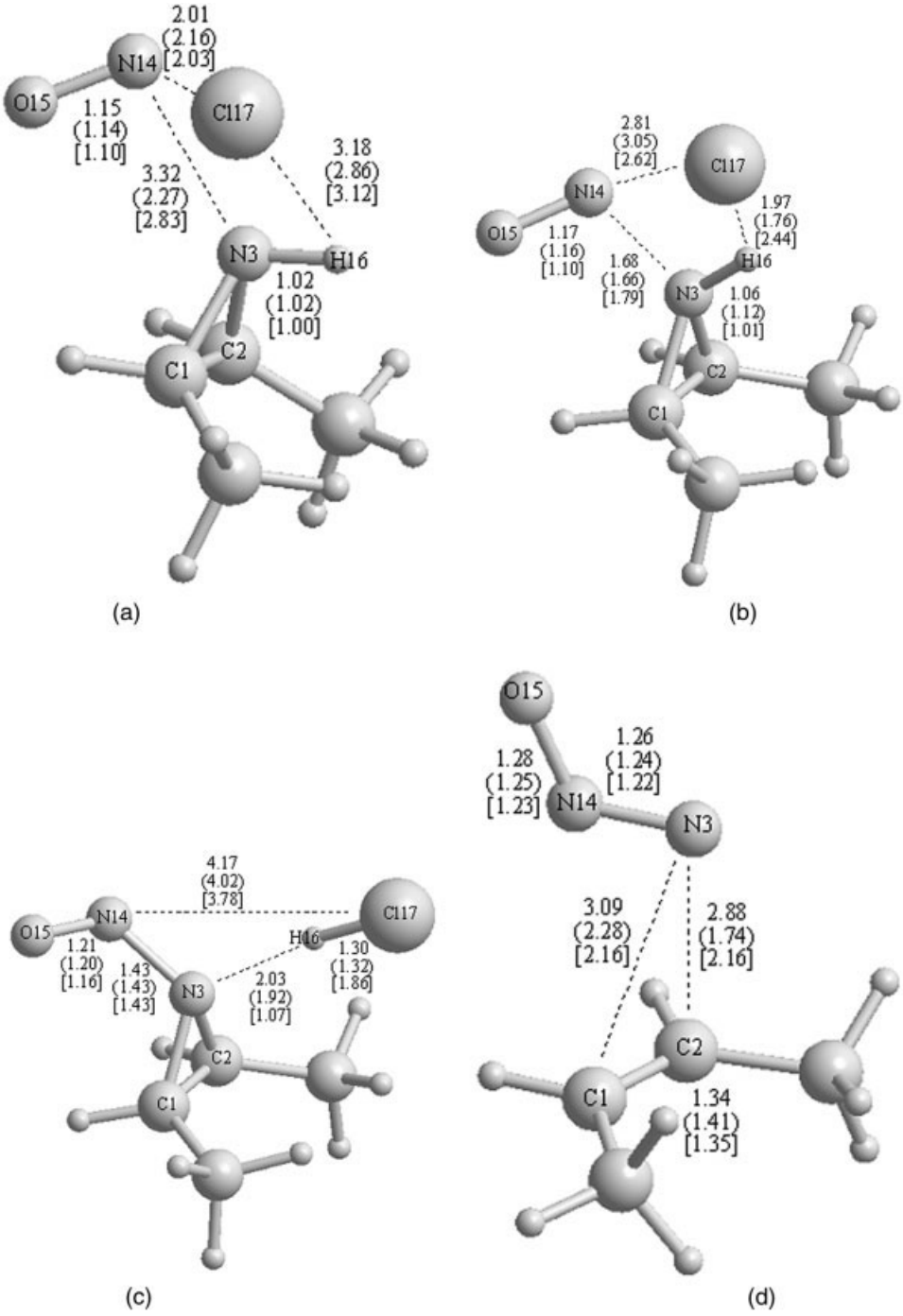


**FIGURE 3.** QCSID/6-31G(d) optimized structures of complexes, transition structures, and intermediates of the deamination of aziridines with NOCl with the most relevant geometric parameters at the QCISD/6-31G(d), (B3LYP/6-31G(d)), and [HF/6-31G(d)] levels of theory for (a) A2, (b) A3, (c) A4, and (d) A5.

the TS2 has a more reactant-like character. This smaller percentage of C–N bond cleaving and the lower formation of alkene and the N=N bond should be the reason for the higher activation energy for this second step at the B3LYP level as compared to QCISD. As the $N_2O$ cleaves from the

**TABLE I**
**Wiberg bond order analysis of deamination of cis aziridines with NOC1 at QCISD/6-31G(d) level.**

| | $BF_j^{Ak}$ | | | $BC_j^{Ak}$ | | | | $BFC_{Ave}^{Ak}$ |
|---|---|---|---|---|---|---|---|---|
| Species | C1–C2 | N3–N14 | H16–Cl17 | C1–N3 | C2–N3 | N3–H16 | N14–Cl17 | N14–O15 | |
| A1 | 0.0 (0.0) | 0.0 (0.0) | 0.0 (0.0) | 0.0 (0.0) | 0.0 (0.0) | 0.0 (0.0) | 0.0 (0.0) | 0.0 (0.0) | 0.0 (0.0) |
| A2 | 0.0 (0.0) | 0.8 (9.0) | 0.0 (0.0) | 1.0 (1.0) | 1.0 (2.0) | 2.4 (5.0) | 6.0 (24.0) | 2.8 (10.0) | 1.8 (6.4) |
| A3 | 0.0 (0.0) | 30.2 (31.0) | 17.2 (38.0) | 6.3 (4.0) | 8.3 (6.0) | 31.8 (42.0) | 92.8 (84.0) | 12.7 (16.0) | 24.9 (27.6) |
| A4 | 0.0 (0.0) | 40.8 (45.0) | 100.0 (100.0) | 4.2 (4.0) | 5.2 (5.0) | 100.0 (100.0) | 100.0 (100.0) | 38.0 (46.0) | 48.5 (50.0) |
| A5 | 97.9 (28.0) | 75.7 (68.0) | 100.0 (100.0) | 97.9 (65.0) | 97.9 (31.0) | 100.0 (100.0) | 100.0 (100.0) | 97.2 (100.0) | 95.8 (74.0) |
| A6 | 100.0 (100.0) | 100.0 (100.0) | 100.0 (100.0) | 100.0 (100.0) | 100.0 (100.0) | 100.0 (100.0) | 100.0 (100.0) | 100.0 (100.0) | 100.0 (100.0) |

B3LYP/6-31G(d) level values are given in parentheses.
For species names and atom labels, refer to Figures 1 and 3.

**TABLE II**
**Complexation energy (kcal · mol$^{-1}$), activation barriers for steps 1 and 2 (kcal · mol$^{-1}$), and reaction energies (kcal · mol$^{-1}$) for the deamination reaction at the B3LYP/6-31G(d) level with different PSs and at HF/6-31G(d) and QCISD/6-31G(d) levels.**

| | | | Activation barriers | | |
|---|---|---|---|---|---|
| PS[a] | $a_o$ | Complexation energy | Step 1 | Step 2 | Reaction energy |
| 1 | 0.200 | 7.42 | 11.75 | 48.81 | 25.00 |
| 2 | 0.000 | 8.87 | 13.04 | 44.36 | 25.45 |
| 3 | 0.100 | 7.64 | 12.96 | 45.75 | 25.97 |
| 4 | 0.200 | 6.51 | 12.51 | 47.09 | 27.49 |
| 5 | 0.300 | 5.57 | 11.95 | 47.15 | 28.19 |
| 6 | 0.400 | 4.92 | 11.48 | 47.40 | 28.73 |
| 7 | 0.500 | 4.57 | 11.21 | 47.91 | 29.15 |
| 8 | 0.600 | 4.32 | 10.96 | 48.56 | 29.46 |
| 9 | 0.700 | 4.20 | 10.85 | 49.25 | 29.67 |
| 10 | 0.800 | 4.03 | 11.10 | 49.92 | 29.79 |
| 11 | 0.900 | 3.91 | 11.61 | 50.58 | 29.81 |
| QCISD | — | 5.35 | 13.87 | 31.09 | 28.13 |
| HF | — | 4.10 | 13.01 | 49.94 | 35.08 |

[a] PS, parameter set, $a_c = a_x$, $a_x = 1 - a_o$, except for PS1, where $a_o = 0.20$, $a_x = 0.72$, and $a_c = 0.81$, the default values for Becke functional in B3LYP calculations.

intermediate A4 in a single step, the stereochemistry is preserved.

Deamination of trans-2,3-dimethylaziridine by NOCl has also been studied at the B3LYP/6-31G(d) level, which also proceeds through the formation of a nitrosoaziridine intermediate and thus the stereochemistry is preserved.

### B3LYP Exact Exchange Reparametrization

Table II lists the complex binding energies, activation energies, and reaction energies for the different species of the reaction computed with the B3LYP hybrid functional, together with 11 different PSs of $a_0$, $a_x$, and $a_c$ derived from the B3LYP functional by varying the exact exchange contribution ($a_0$), together with the HF and QCISD results for comparison.

By taking the QCISD results as the reference, it is seen that the HF method underestimates the complex binding energy and B3LYP overestimates it, while PS5 gives the best results. However, for the activation barrier of step 1, HF performs surprisingly far better than B3LYP. Here the increase of the

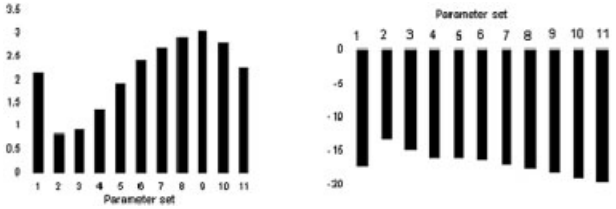


**FIGURE 4.** Difference between the energy barriers provided by each parameter set at the B3LYP/6-31G(d) level and that obtained at QCISD/6-31G(d) method: (a) Step 1; (b) Step 2.

$a_o$ value results in a general decrease of the energy barrier. For the second step, both the HF and B3LYP methods overestimate the energy barrier, and PS2, with $a_o = 0$, performs relatively better than other PSs, although a possible difference exists (~13 kcal · $mol^{-1}$) with respect to QCISD. Figure 4 is a graphical representation of energy differences between QCISD and other PSs values. Here the increase in energy barrier is observed with the increase of $a_0$, opposite to step 1. On the whole, after all the PSs studied, PS2 with $a_o = 0$, i.e., the BLYP method, is the one that provides better energy barriers, although still far from the QCISD results. The reaction energy provided by PS5 is much closer to the QCISD energy, while B3LYP gives somewhat underestimated results. In this case, HF calculation overestimates the exothermicity, while in DFT it increases with the increase of $a_o$. Summarizing, the amount of exact exchange included in Becke's B3LYP functional calculations have a noticeable influence on the computed activation and reaction energies, but in contrast to previous results [7], a pure DFT functional such as BLYP performs better than hybrid DFT functionals for energy barriers.

## Conclusions

Deamination of cis and trans-2,3-dimethylaziridines using NOCl results in the formation of dimethyl alkenes with the same stereochemistry. Calculations reveal that the reaction is totally stereospecific and takes place in two steps. In the first step, a pre-reactive complex is formed followed by a spiro-type TS. This TS undergoes dissociative cycloelimination to form the intermediate N-nitrosoaziridine and HCl, in agreement with experimental results. In the second step, N-nitrosoaziridine undergoes cycloreversion in a concerted way to form the respective alkenes. Formation of N-nitrosoaziridine intermediate and the cleavage of this in a single step lead to the stereochemical retention and it is the rate-determining step. Computed activation energies for steps 1 and 2 at the QCISD level are found to be 13.87 and 31.09 kcal · $mol^{-1}$, respectively. The HF and B3LYP methods overestimate the second barrier for the rate-determining step. Computed bond indices describe very well the bond formation and bond breaking in the reaction path. A systematic study of the effect of the exact exchange in B3LYP calculations on the energy barriers and reaction energies of this reaction was also carried out. The BLYP, which is the pure functional with 0% exact exchange, is found to perform better than B3LYP for the activation barriers calculation, whereas the functional with 30% exact exchange gets closer to QCISD when calculating the complexation and reaction energies.

## Supporting Information Available

HF/6-31G(d), B3LYP/6-31G(d), and QCISD/6-31G(d) optimized Cartesian coordinates of reactants, complex, transition states, intermediates, and products with total energies (hartrees) is available free of charge via the Internet at http://www.interscience.wiley.com/jpages/0020-7608/suppmat.

## References

1. Sonnet, P. E. Tetrahedron 1980, 36, 557.
2. Tanner, D. Angew Chem Int Ed Engl 1994, 33, 559.
3. Ham, G. E. J Org Chem 1964, 29, 3052. Vicario, J. L.; Badia D.; Carrillo, L. J Org Chem 2001, 66, 5801.
4. Clark, R. D.; Helmkamp, G. K. J Org Chem 1964, 29, 1316.
5. Becke, A. D. J Chem Phys 1993, 98, 5648.
6. Latajka, Z.; Bouteiller, Y.; Scheiner, S. Chem Phys Lett 1995, 234, 159. Lundell, J.; Latajka, Z. J Phys Chem A 1997, 101, 5004.
7. Poater, J.; Solà, M.; Duran, M.; Robles, J. Phys Chem Chem Phys 2002, 4, 722.
8. Chermette, H.; Razafinjanahary, H.; Carrion, L. J Chem Phys 1997, 107, 10643.
9. Hoe, W.-M.; Cohen, A. J.; Handy, N. C. Chem Phys Lett 2001, 341, 319.
10. Csonka, G. I.; Nguyen, N. A.; Kolossváry, I. J Comput Chem 1997, 18, 1534.
11. Solà, M.; Forés, M.; Duran, M. In Advances in Molecular Similarity; Carbó, R. Mezey, P. Eds.; JAI Press: New York, 1998, Vol. 2, p 187.
12. Poater, J.; Duran, M.; Solà, M. J Comput Chem 2001, 22, 1666.

13. Durant, J. L. Chem Phys Lett 1996, 256, 595.
14. Jursic, B. S. In Recent Developments and Applications of Modern Density Functional Theory; Seminario, J. M., Ed.; Elsevier Science: Amsterdam, 1996; p 709.
15. Lynch, B. J.; Fast, P. L.; Harris, M.; Truhlar, D. G. J Phys Chem A 2000, 104, 4811. Lynch, B. J.; Truhlar, D. G. J Phys Chem A 2001, 105, 2936.
16. Kormos, B. L.; Cramer, C. J. J Phys Org Chem 2002, 15, 712.
17. Abu-Awwad, F.; Politzer, P. J Comput Chem 2000, 21, 227.
18. Dkhissi, A.; Alikhani, M. E.; Boutellier, Y. J Mol Struct (Theochem)1997, 416, 1.
19. Wilson, P. J.; Tozer, D. J. J Chem Phys 2002, 116, 10139.
20. Pople, J. A.; Gordon, M. H.; Raghavachari, K. J Chem Phys 1987, 87, 5968.
21. Lee, C.; Yang, W.; Parr, R. G. Phys Rev B 1988, 37, 785.
22. Frisch, M. J.; Trucks, G. W.; Schlegel, H. B.; Scuseria, G. E.; Robb, M. A.; Cheeseman, J. R.; Zakrzewski, V. G.; Montgomery, J. A.; Stratmann, R. E.; Burant, J. C.; Dapprich, S.; Millam, J. M.; Daniels, A. D.; Kudin, K. N.; Strain, M. C.; Farkas, O.; Tomasi, J.; Barone, V.; Cossi, M.; Cammi, R.; Mennucci, B.; Pomelli, C.; Adamo, C.; Clifford, S.; Ochterski, J.; Petersson, G. A.; Ayala, P. Y.; Cui, Q.; Morokuma, K.; Salvador, P.; Dannenberg, J. J.; Malick, D. K.; Rabuck, A. D.; Raghavachari, K.; Foresman, J. B.; Cioslowski, J.; Ortiz, J. V.; Baboul, A. G.; Stefanov, B. B.; Liu, G.; Liashenko, A.; Piskorz, P.; Komaromi, I.; Gomperts, R.; Martin, R. L.; Fox, D. J.; Keith, T.; Al-Laham, M.; Peng, C.; Nanayakkara, A.; Challacombe, M.; Gill, P. M. W.; Johnson, B. G.; Chen, W. Wong, M. W.; Andres, J. L.; Gonzalez, R.; Head-Gordon, M.; Replogle, E. S.; Pople, J. A. Gaussian 98, rev. A11, Pittsburgh, PA, 1998.
23. Frisch, M. J.; Pople, J. A.; Binkley, J. S. J Chem Phys 1984, 80, 3265.
24. Schaftenaar, G.; Noordik, J. H. J Comput Aid Mol Design 2000, 14, 123.
25. Wiberg, K. Tetrahedron 1968, 24, 1083.
26. Reed, A. E.; Curtiss, L. A.; Weinhold, F. Chem Rev 1988, 88, 889. Foster J. P.; Weinhold, F. J Am Chem Soc 1980, 102, 7211.
27. Manoharan, M.; Venuvanalingam, P. J Mol Struct (Theochem) 1997, 394, 41. Manoharan, M.; Venuvanalingam, P. J Chem Soc Perkin Trans 2 1996, 1423. Manoharan, M.; Venuvanalingam, P. J Chem Soc Perkin Trans 2 1997, 1799.
28. Stephens, P. J.; Devlin, F. J.; Chabalowski, C. F.; Frisch, M. J. J Phys Chem 1994, 98, 11623.
29. Becke, A. D. Phys Rev A 1988, 38, 3098.
30. Becke, A. D. J Chem Phys 1996, 104, 1040.